

Supplementary Information

Phase transitions and microstructure of ferroelastic MIEC oxide $\text{SrCo}_{0.8}\text{Fe}_{0.2}\text{O}_{2.5}$ doped with highly charged cations Nb/Ta(V).

Irina V. Belenkaya^a, Alexandr A. Matvienko^{ab}, Alexandr P. Nemudry^{ab*}

^aInstitute of Solid State Chemistry and Mechanochemistry, SB RAS; 630128 Kutateladze 18,
Novosibirsk, Russia

^bNovosibirsk State University; 630090 Pirogova 2, Novosibirsk, Russia

S1. Isostoichiometric mode.

In the isostoichiometric mode in order to maintain constant oxygen stoichiometry the necessary oxygen partial pressure ($p\text{O}_2$) was produced for each temperature with the help of gas mixture unit UFNGS (SoLo) in agreement with the obtained phase diagrams. The values of $p\text{O}_2$ are listed in Table S1.

Table S1. Temperature and $p\text{O}_2$ corresponding to the isostoichiometric mode for $\text{SrCo}_{0.8-x}\text{Fe}_{0.2}\text{Nb}_x\text{O}_{3-\delta}$ oxides ($x=0, 0.02, 0.05$) with $3-\delta = 2.5, 2.52$ and 2.55 , respectively.

$\text{SrCo}_{0.8}\text{Fe}_{0.2}\text{O}_{2.5}$		$\text{SrCo}_{0.78}\text{Fe}_{0.2}\text{Nb}_{0.02}\text{O}_{2.52}$		$\text{SrCo}_{0.75}\text{Fe}_{0.2}\text{Nb}_{0.05}\text{O}_{2.55}$	
T, °C	$p\text{O}_2$, atm	T, °C	$p\text{O}_2$, atm	T, °C	$p\text{O}_2$, atm
700	1.7×10^{-3}	600	1.9×10^{-4}	500	1.1×10^{-4}
730	8.5×10^{-3}	625	1.9×10^{-3}	525	1.7×10^{-4}
740	8.5×10^{-3}	650	3.5×10^{-3}	550	2.8×10^{-4}
750	8×10^{-3}	675	1.4×10^{-3}	575	3.5×10^{-4}
760	4.4×10^{-3}	700	6.6×10^{-4}	600	2.8×10^{-4}
770	1.9×10^{-3}	725	7.4×10^{-4}	625	3.5×10^{-4}
780	1.5×10^{-3}	750	1.3×10^{-3}	650	7.4×10^{-4}
800	3×10^{-3}	800	4.5×10^{-3}	700	3.6×10^{-3}
900	5.5×10^{-2}	900	3×10^{-2}	900	1.1×10^{-1}

* Corresponding author. Tel.: +7 383 233 24 10 * 1183, fax: +7 383 332 28 47, email: nemudry@solid.nsc.ru

Table S2. Refined atomic positions in the crystal structure of T phase having the composition $\text{SrCo}_{0.8}\text{Fe}_{0.2}\text{O}_{2.5}$ at 780°C and $p\text{O}_2=1.5 \times 10^{-3}$ atm. Space group P4/mmm (№123) $a_T=3.9453(1)\text{\AA}$, $c_T=7.9107(2)\text{\AA}$.

Atom	x	y	z	Occupancy
Sr	0.5	0.5	0.2589	1
Co/Fe(1)	0	0	0	0.8/0.2
Co/Fe(2)	0.999	0.0026	0.5	0.1/0.025
O(1)	0.5	0	0	1
O(2)	0	0	0.245	1
O(3)	0	0.5025	0.5	0.25

Table S3. The ratios between T and BM phases depending on temperature for $\text{SrCo}_{0.8-x}\text{Fe}_{0.2}\text{Nb}_x\text{O}_{2.5+x}$ ($x=0$; 0.2) oxides.

$\text{SrCo}_{0.8}\text{Fe}_{0.2}\text{O}_{2.5}$			$\text{SrCo}_{0.78}\text{Fe}_{0.2}\text{Nb}_{0.02}\text{O}_{2.52}$		
Temperature, °C	Phase relations		Temperature, °C	Phase relations	
	T	BM		T	BM
770	100	0	725	100	0
760	76	24	700	94	6
750	46	54	675	89	11
740	13	87	650	80	20
730	5	95	625	10	90
700	0	100	600	0	100

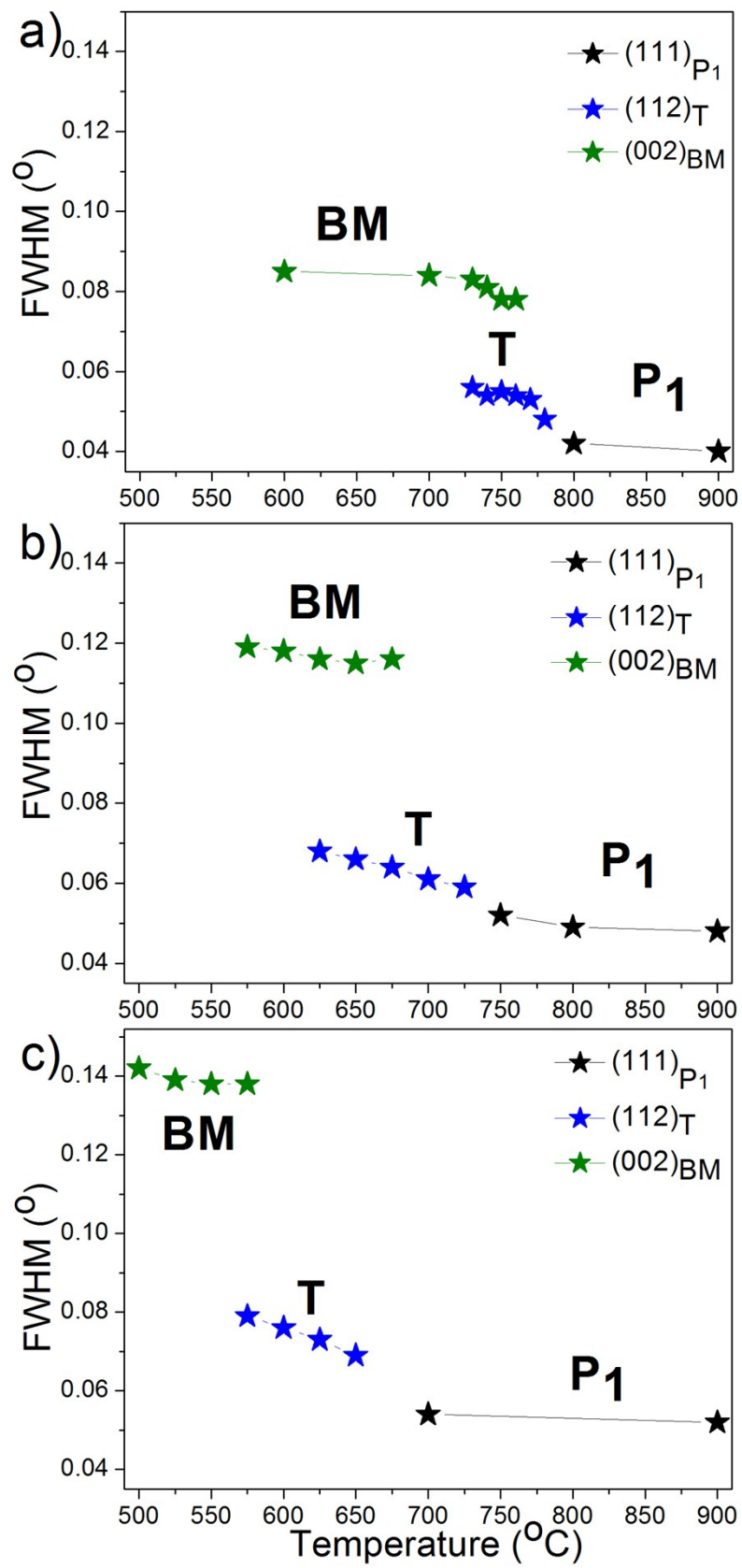


Figure S1. FWHM of reflections: (111) in P₁ phase, (112) in T phase, (002) in BM phase for (a) SrCo_{0.8}Fe_{0.2}O_{2.5}, (b) SrCo_{0.78}Fe_{0.2}Nb_{0.02}O_{2.52}, (c) SrCo_{0.75}Fe_{0.2}Nb_{0.05}O_{2.55} oxides, studied in the isostoichiometric mode.

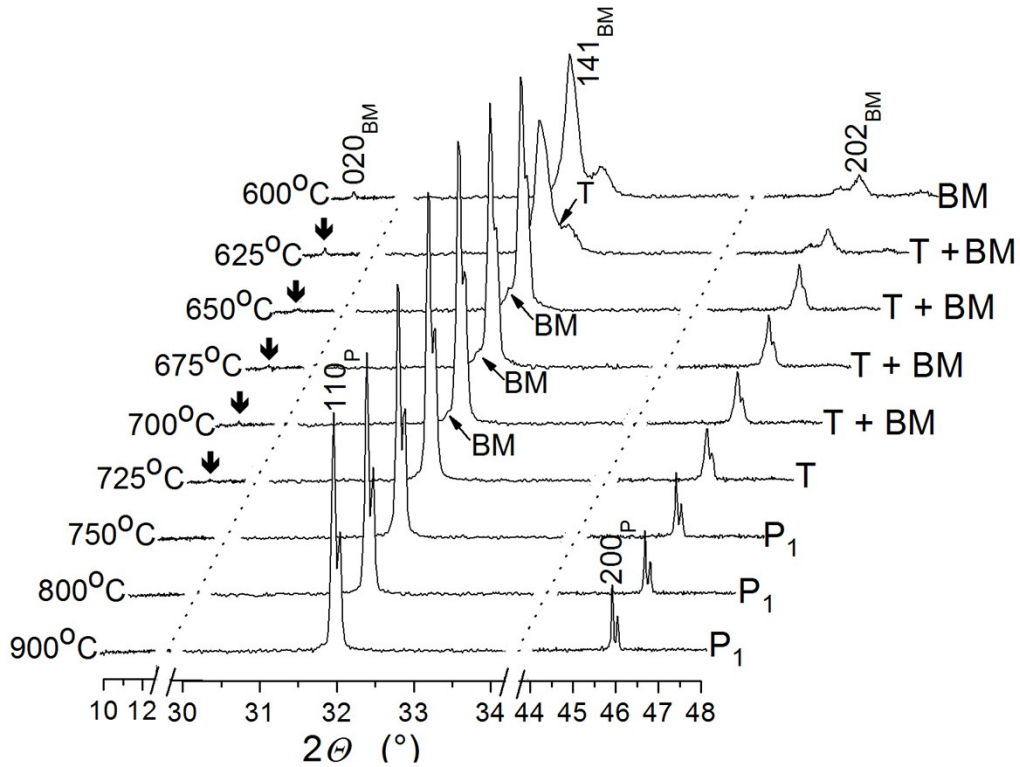


Figure S2. Fragments of *in situ* HT XRD patterns of $\text{SrCo}_{0.78}\text{Fe}_{0.2}\text{Nb}_{0.02}\text{O}_{2.52}$ oxide at different temperatures in the isostoichiometric mode. Characteristic reflections of the phase T at $2\Theta \sim 11^\circ$ are marked by arrows ↗.

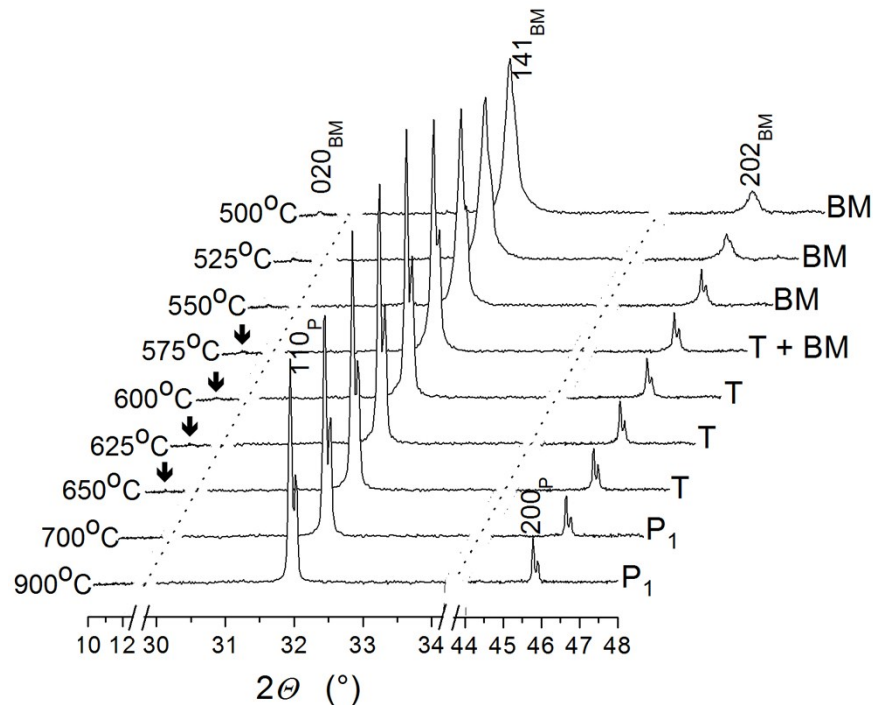


Figure S3. Fragments of *in situ* HT XRD patterns of $\text{SrCo}_{0.75}\text{Fe}_{0.2}\text{Nb}_{0.05}\text{O}_{2.55}$ oxide at different temperatures in the isostoichiometric mode. Characteristic reflections of the phase T at $2\Theta \sim 11^\circ$ are marked by arrows ↗.

S2. Isobaric mode.

The perovskite-brownmillerite phase transition in $\text{SrCo}_{0.8-x}\text{Fe}_{0.2}\text{M}_x\text{O}_{2.5+y}$ compounds ($\text{M} = \text{Nb}, \text{Ta}; 0 \leq x \leq 0.1; y \sim x$) was studied at different temperatures in the isobaric mode ($p\text{O}_2 \sim 5 \times 10^{-4}$ atm). According to the obtained data the phase transition from brownmillerite to perovskite in $\text{SrCo}_{0.8-x}\text{Fe}_{0.2}\text{M}_x\text{O}_{2.5+y}$ ($\text{M} = \text{Nb}, \text{Ta}; 0 \leq x \leq 0.05$) in the isobaric mode proceeds in two stages too: $\text{P}_{1,2} \rightarrow \text{T} \rightarrow \text{BM}$. The first stage involves the formation of the intermediate tetragonal phase T, which is characterized by reflection splitting at $2\Theta \sim 32^\circ$ (110_p), 46° (200_p), 57° (211_p) and the formation of additional low-intensity reflections at $2\Theta \sim 11^\circ, 25^\circ, 41^\circ, 48^\circ$ (Figures S4-S6). At the second stage, in the two-phase mode the transition into the phase with brownmillerite structure occurs. Similarly to the isostoichiometric mode, an increase in dopant concentration is accompanied by a decrease in the temperature of phase transition and leads to the elimination of tetragonal and orthorhombic distortions of lattices and a decrease in size of coherent scattering regions (CSR) of the phase with brownmillerite structure (Figure S7).

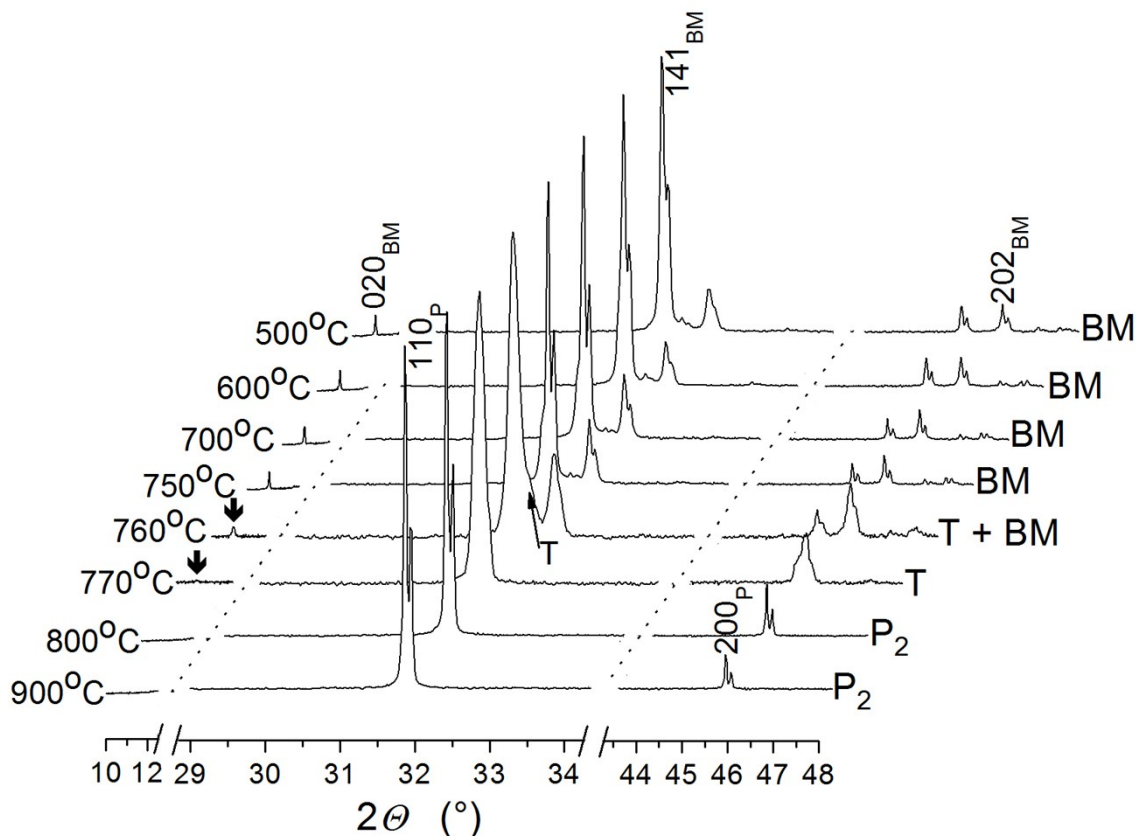


Figure S4. Fragments of *in situ* HT XRD patterns of $\text{SrCo}_{0.8}\text{Fe}_{0.2}\text{O}_{2.5+y}$ oxide at different temperatures in the isobaric mode. Characteristic reflections of the phase T at $2\Theta \sim 11^\circ$ are marked by arrows ↗.

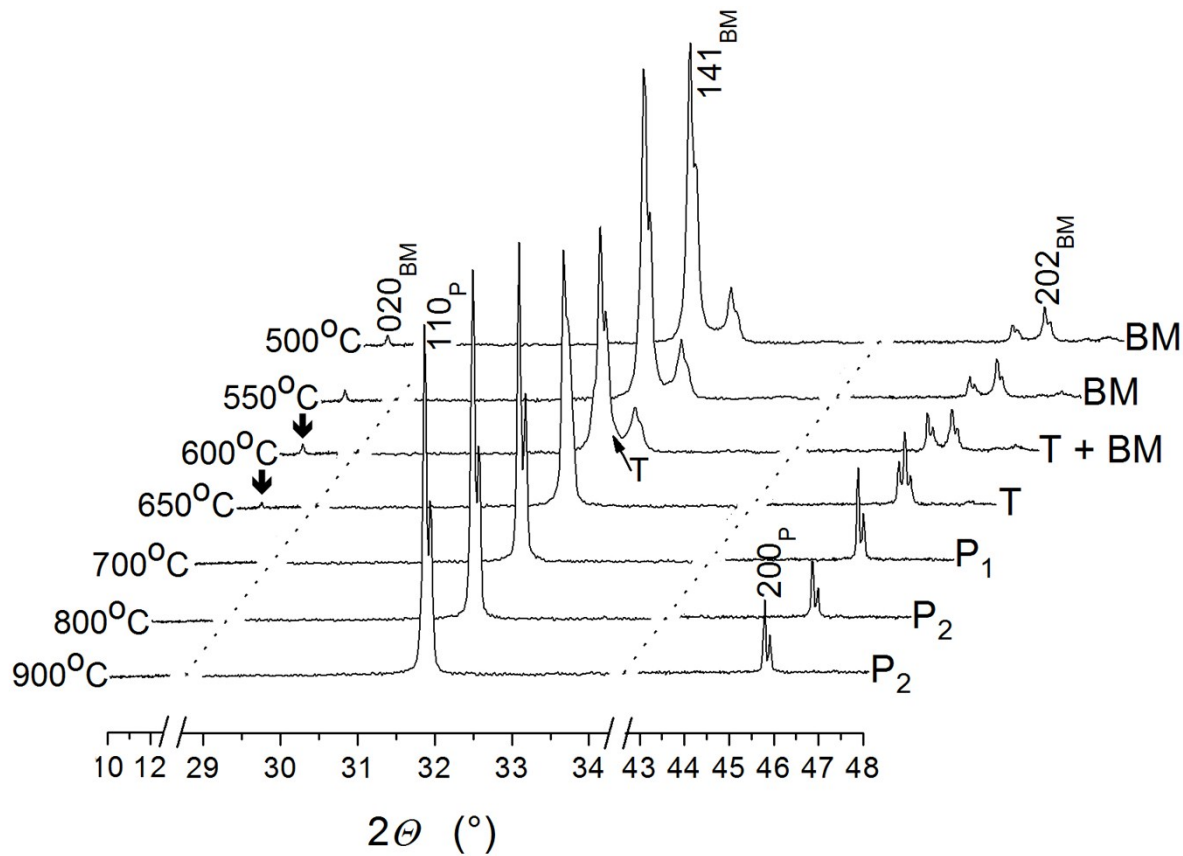


Figure S5. Fragments of *in situ* HT XRD patterns of $\text{SrCo}_{0.78}\text{Fe}_{0.2}\text{Nb}_{0.02}\text{O}_{2.5+y}$ oxide at different temperatures in the isobaric mode. Characteristic reflections of the phase T at $2\Theta \sim 11^\circ$ are marked by arrows ↗.

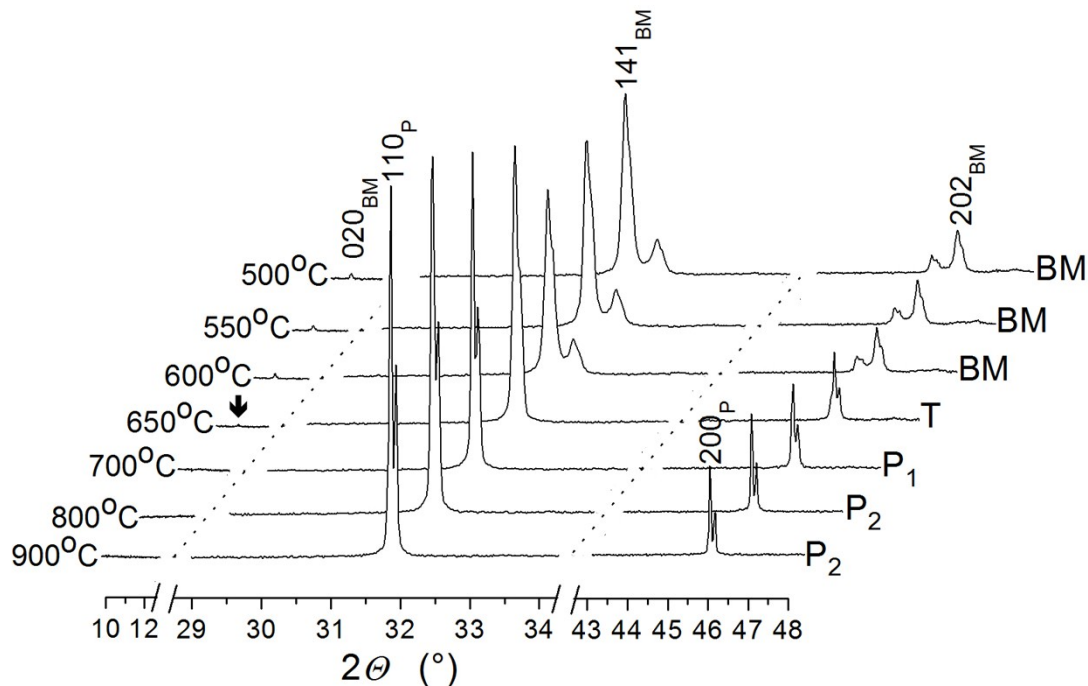


Figure S6. Fragments of *in situ* HT XRD patterns of $\text{SrCo}_{0.75}\text{Fe}_{0.2}\text{Nb}_{0.05}\text{O}_{2.5+y}$ oxide at different temperatures in the isobaric mode. Characteristic reflections of the phase T at $2\Theta \sim 11^\circ$ are marked by arrows ↗.

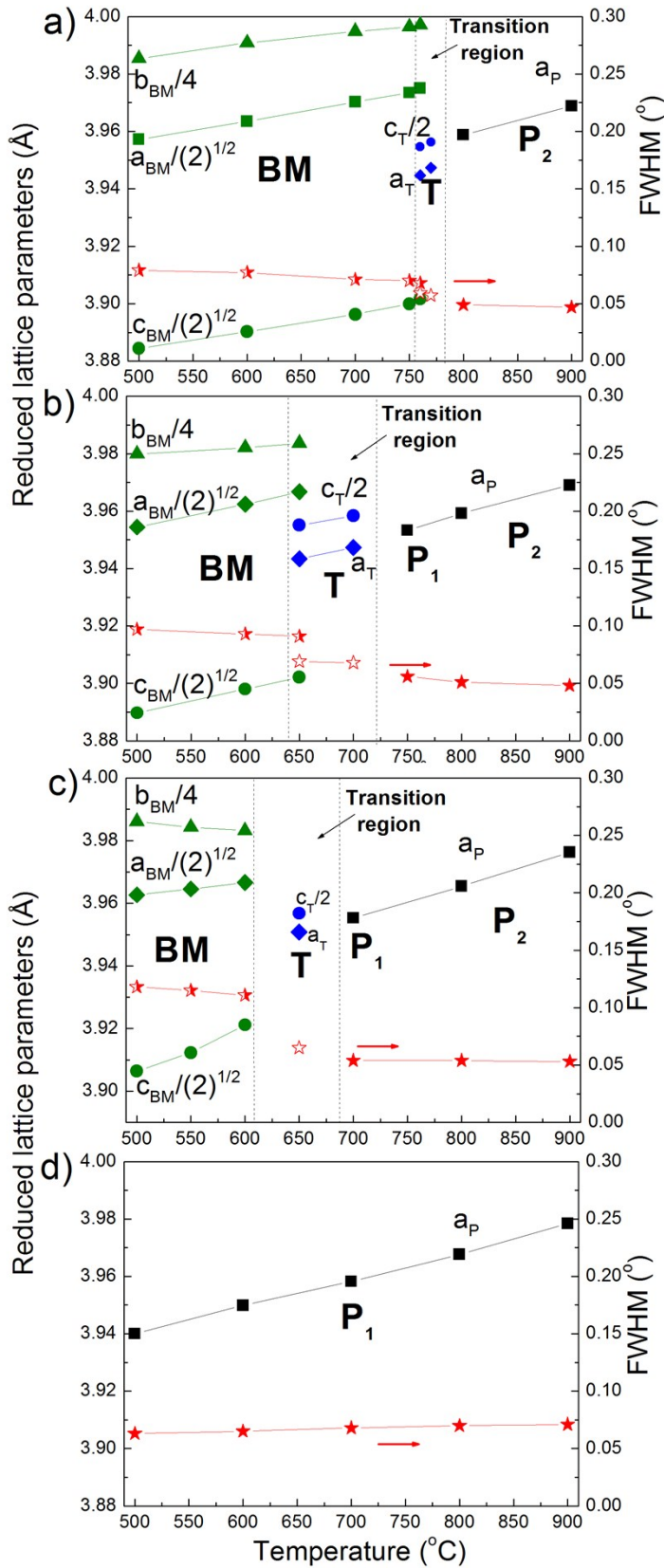


Figure S7. Reduced lattice parameters of $\text{P}_{1,2}$, T and BM phases, and integral widths of reflections: (111) in $\text{P}_{1,2}$ phase (\star), (112) in T phase (\star), (002) in BM phase (\blacktriangledown) for compounds (a) $\text{SrCo}_{0.8}\text{Fe}_{0.2}\text{O}_{2.5\pm y}$, (b) $\text{SrCo}_{0.78}\text{Fe}_{0.2}\text{Nb}_{0.02}\text{O}_{2.5\pm y}$, (c) $\text{SrC}_{0.75}\text{Fe}_{0.2}\text{Nb}_{0.05}\text{O}_{2.5\pm y}$, (d) $\text{SrC}_{0.7}\text{Fe}_{0.2}\text{Nb}_{0.1}\text{O}_{2.5\pm y}$ studied in the isobaric mode.

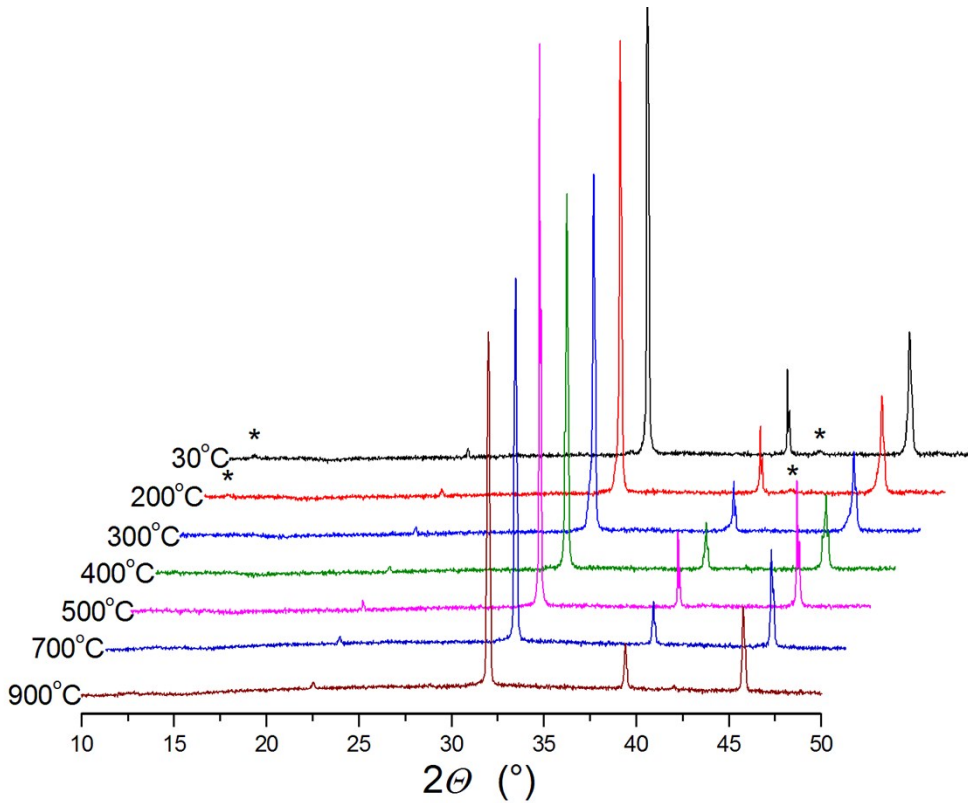


Figure S8. Fragments of *in situ* HT XRD patterns of $\text{SrCo}_{0.7}\text{Fe}_{0.2}\text{Nb}_{0.1}\text{O}_{2.5+y}$ oxide at different temperatures in the isobaric mode. Asterisks mark the weak diffuse maxima.

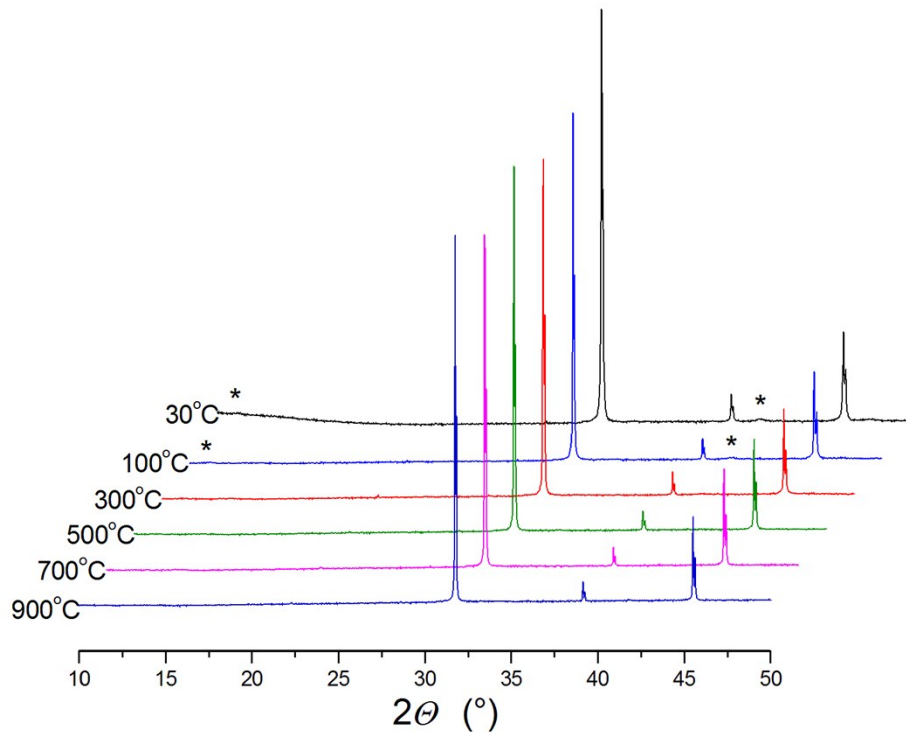


Figure S9. Fragments of *in situ* HT XRD patterns of $\text{SrCo}_{0.7}\text{Fe}_{0.2}\text{Ta}_{0.1}\text{O}_{2.5\pm y}$ oxide at different temperatures in the isobaric mode. Asterisks mark the weak diffuse maxima.

S3. Structure of low-temperature $\text{SrCo}_{0.8-x}\text{Fe}_{0.2}\text{Nb}_x\text{O}_{2.5+y}$ phases ($0 \leq x \leq 0.1$; $y \sim x$).

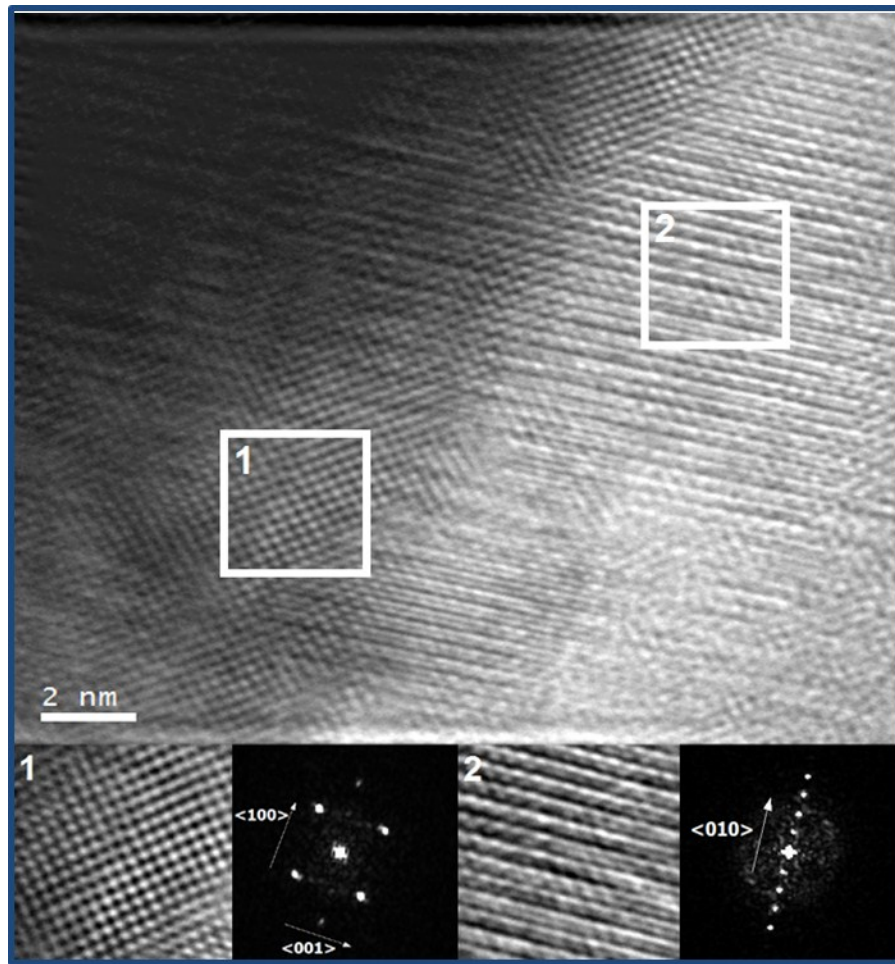


Figure S10. Data of transmission electron microscopy and the corresponding diffraction patterns obtained by fast Fourier transform of the selected regions for $\text{SrCo}_{0.7}\text{Fe}_{0.2}\text{Nb}_{0.1}\text{O}_{2.58}$, demonstrating the formation of 90° twins with brownmillerite structure.

Mössbauer spectra of $\text{SrCo}_{0.8-x}\text{Fe}_{0.2}\text{M}_x\text{O}_{2.5+y}$ oxides ($\text{M}=\text{Nb}, \text{Ta}; 0.05 < x \leq 0.1$) at room temperature are composed of two magnetically ordered components (Figure S10, Table S4), corresponding to Fe^{3+} ions in octahedral and tetrahedral positions, which is characteristic of brownmillerite structure, and paramagnetic component of Fe^{3+} ions in pentahedral sites. The presence of paramagnetic component in the spectrum related to the presence of perovskite phase. The data obtained by means of Mössbauer spectroscopy confirm the formation of specific microstructure based on brownmillerite structure in the doped samples with $0.05 < x \leq 0.1$.

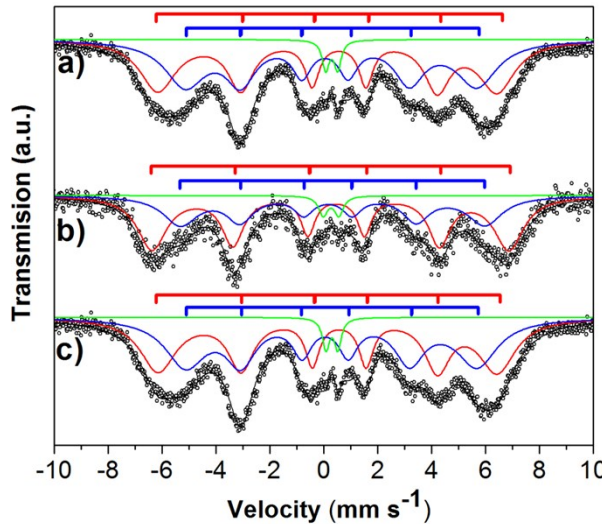


Figure S11. Mössbauer spectra of compounds (a) $\text{SrCo}_{0.73}\text{Fe}_{0.2}\text{Ta}_{0.07}\text{O}_{2.58}$, (b) $\text{SrCo}_{0.7}\text{Fe}_{0.2}\text{Ta}_{0.1}\text{O}_{2.6}$ and (c) $\text{SrCo}_{0.7}\text{Fe}_{0.2}\text{Nb}_{0.1}\text{O}_{2.58}$. The red line corresponds to Fe^{3+} ions in octahedral sites, the blue line corresponds to Fe^{3+} ions in tetrahedral sites, the green line corresponds to paramagnetic component of Fe^{3+} ions in pentahedral sites.

Table S4. Parameters of Mössbauer spectra of low-temperature phases of perovskite-like oxides $\text{SrCo}_{0.8-x}\text{Fe}_{0.2}\text{M}_x\text{O}_{2.5+y}$ ($\text{M} = \text{Nb}, \text{Ta}; 0.05 < x \leq 0.1, y \sim x$) at room temperature.

Sample	Iron State	IS (mm/s)	QS (mm/s)	FWHM (mm/s)	B (T)	I (%)
$\text{SrCo}_{0.73}\text{Fe}_{0.2}\text{Ta}_{0.07}\text{O}_{2.58}$	$\text{Fe}^{3+}(\text{O})$	0.36	-0.21	0.46	12.58	49
	$\text{Fe}^{3+}(\text{T})$	0.17	0.11	0.68	10.58	48
	$\text{Fe}^{3+}(\text{P})$	0.3	0.44	0.31	-	3
$\text{SrCo}_{0.7}\text{Fe}_{0.2}\text{Ta}_{0.1}\text{O}_{2.6}$	$\text{Fe}^{3+}(\text{O})$	0.35	-0.11	0.50	13.24	50
	$\text{Fe}^{3+}(\text{T})$	0.24	0.09	0.71	11.30	46
	$\text{Fe}^{3+}(\text{P})$	0.26	0.58	0.41	-	4
$\text{SrCo}_{0.7}\text{Fe}_{0.2}\text{Nb}_{0.1}\text{O}_{2.58}$	$\text{Fe}^{3+}(\text{O})$	0.34	-0.23	0.49	12.65	49
	$\text{Fe}^{3+}(\text{T})$	0.17	0.09	0.71	10.74	47
	$\text{Fe}^{3+}(\text{P})$	0.31	0.46	0.33	-	4

S4. Structure of high-temperature $\text{SrCo}_{0.8-x}\text{Fe}_{0.2}\text{M}_x\text{O}_{2.5+y}$ phases ($\text{M} = \text{Nb}, \text{Ta}; 0 \leq x \leq 0.1$).

Table S5. Parameters of Mössbauer spectra of $\text{SrCo}_{0.77}\text{Fe}_{0.2}\text{Ta}_{0.03}\text{O}_{2.51}$ recorded at different temperatures at constant $p\text{O}_2$.

Temperature, °C	Fe ³⁺ in octahedral positions			Fe ³⁺ in tetrahedral positions		
	IS (mm/s)	QS (mm/s)	I (%)	IS (mm/s)	QS (mm/s)	I (%)
450	0.08	1.09	48	-0.15	1.12	52
600	0.02	0.75	45	-0.22	0.67	55
700	-0.08	0.36	45	-0.25	0.36	55